Magnetism of manganese in RMn_2 and RMn_4Al_8 (R = Y, Gd, Er) intermetallics

1998 J. Phys.: Condens. Matter 10 581

(http://iopscience.iop.org/0953-8984/10/3/011)

J. Phys.: Condens. Matter **10** (1998) 581–592. Printed in the UK PII: S0953-8984(98)82518-6

Magnetism of manganese in RMn_2 and RMn_4Al_8 (R = Y, Gd, Er) intermetallics

E Talik†, M Neumann†‡, T Mydlarz†§, J Kusz†, H Böhm†‖, A Winiarski† and A Gilewski†§

† Institute of Physics, University of Silesia, Universytecka 4, 40-007 Katowice, Poland
‡ Universität Osnabrück, Fachbereich Physics, Barbarastr. 7, 49069 Osnabrück, Germany
§ International Laboratory of High Fields and Low Temperatures, Gajowicka 95, 53-529 Wrocław, Poland
‖ Institut für Geowissenschaften der Universität, Saarstr. 21, 55099 Mainz, Germany

Received 4 July 1997

Abstract. The XPS electronic structure was measured for YMn_2, $GdMn_2$, $ErMn_2$, YMn_4Al_8 and $GdMn_4Al_8$ single crystals and pure Mn. Exchange splitting of Mn 3d and 3s states was found for the compounds with magnetic manganese. The electrical resistivity of the $GdMn_2$ single crystal shows an antiferromagnetic transition at 108 K and the second transition at 32 K. The lattice parameter against temperature of $GdMn_2$ exhibits a large spontaneous magnetostriction at T_N. The anisotropic character of the $GdMn_2$ magnetization was found. The results were discussed using the Yamada and Shimizu model.

1. Introduction

The magnetic properties of the intermetallic compounds R–T (R—rare earth element, T—transition metal 3d, 4d, 5d) have recently been examined intensively. RMn_2 crystallizes in the cubic C15 Laves phase (for R = Y, Gd, Tb and Dy) or the hexagonal C14 Laves phase (for R = Pr, Nd, Sm, Er, Tm and Lu). $HoMn_2$ has both structures depending on the heat treatment [1]. RMn_2 with a magnetic rare earth element consists of two magnetic sublattices which are formed by the localized 4f electrons of R and the itinerant 3d electrons of Mn. The Mn magnetism is close to the instability limit due to a critical value of the Mn–Mn interatomic distances ($d_c = 2.67$ Å at 4.2 and 2.7 Å at 300 K) which lead to a huge magnetovolume anomaly [2, 3]. Both YMn_2 and $GdMn_2$ have a similar Mn–Mn distance which is larger than the critical d_c which leads to the stability of the Mn moments [4]. YMn_2 is an antiferromagnet with a helical modulation which was concluded from a neutron diffraction experiment [5]. It exhibits a giant volume change at T_N related to the transition from spin fluctuations to a local moment of Mn [6]. For $GdMn_2$ the magnetic structure is not established by the neutron experiment due to strong neutron absorption by Gd [7]. For the single crystals of the RMn_2 compounds obtained by Makihara *et al* [8], using the Bridgman method, the measurements of the magnetization, ac susceptibility and the electrical resistivity were performed. They concluded the simple ferrimagnetic structure for $GdMn_2$. Ibarra *et al* [9] suggested a co-existence of two phases below T_N: a transformed one, in which the magnetic moment of Mn is stable, and a non-transformed one, in which the magnetic moment is not present. Moreover they concluded an ordering of the Gd sublattice

0953-8984/98/030581+12$19.50

below T_c (about 35 K). The separate ordering of the Gd sublattice was not confirmed by Mössbauer, NMR and specific heat measurements [10–12]. Przewoźnik [10] and Żukrowski [13] concluded from Mössbauer measurements the ordering of the Gd sublattice also above 40 K even up to T_N. Yoshimura *et al* [11] found a perpendicular alignment of the Gd and Mn moments and an antiferromagnetic coupling between the Mn moments from the NMR measurements. Yamada and Shimizu [14–16] have deduced from their calculations that the moments of Mn in $GdMn_2$ are canted by the hybridizations between 3d states of Mn and 5d states of Gd and by the exchange field created by the localized moments of Gd. Recently Hauser *et al* [17] concluded from the thermal expansion measurements that a separate magnetic ordering of the Gd and Mn sublattices which can be induced by external pressure should occur.

YMn_4Al_8 and $GdMn_4Al_8$ crystallize in the tetragonal $ThMn_{12}$ crystal structure. For this structure the manganese atoms occupy mainly the 8f sites with the Mn–Mn distance $d = 2.56$ Å [18] which is below the critical one. For such a small distance the manganese atoms do not carry the magnetic moment.

The aim of this work is to compare the electronic structure of RMn_2 and RMn_4Al_8 single crystals and the electrical resistivity, magnetic susceptibility, magnetization and lattice parameter measurements for a better understanding of the problem of Mn magnetism.

2. Experimental details

The YMn_2, $GdMn_2$, $ErMn_2$, YMn_4Al_8 and $GdMn_4Al_8$ single-crystalline samples were obtained by the Czochralski method from a levitated melt [19] using high-purity starting materials. To avoid formation of R_6Mn_{23} a small excess of rare earth was added (about 3%) to the nominal stoichiometry. The quality of the samples was checked by x-ray methods. The compounds were identified by the x-ray powder diffraction with Cu Kα radiation using a Siemens D-5000 diffractometer. The Berg–Barrett x-ray topography of $GdMn_2$ (figure 1) shows that the investigated crystal is a good quality single crystal without a mosaic structure. The changes of contrast in the topography are due to roughness of the 'as-grown' crystal surface.

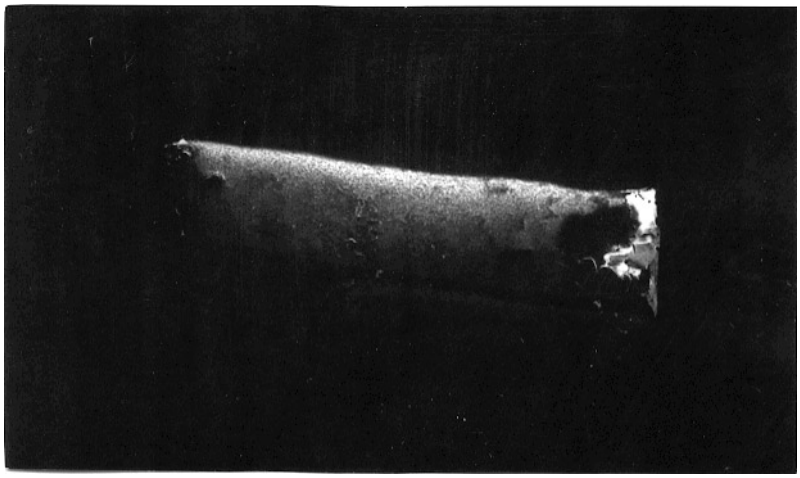

Figure 1. X-ray Berg–Barrett topography of a $GdMn_2$ single crystal; (440) reflection.

Single crystals of $GdMn_2$ of good quality of the approximate size of 0.5 mm × 0.5 mm × 0.5 mm were studied using the graphite–monochromatized Cu Kα radiation (Enraf–Nonius rotating anode) and a four-circle diffractometer with 250 mm χ-circle (Huber) controlled by a PC with the STOE STADI4 program system and equipped with a two-stage closed-cycle helium low-temperature attachment (CTI Cryogenics). The temperature was controlled within 0.1 K. The refinement of cell parameters was carried out by measuring about 60 reflections with high 2Θ-values and their Friedel pairs at both sides of the primary beam. An ω-scan was carried out at + and −2Θ and ω. The centre of gravity was determined for both scans and the observed 2Θ value was determined by the difference of the two ω centres [20]. These results are free of zero-point errors, absorption effects and systematic errors resulting from miscentring of the crystal.

The XPS spectra of YMn_2, $GdMn_2$, $ErMn_2$, YMn_4Al_8, $GdMn_4Al_8$, pure Mn and Gd at room temperature were obtained with monochromatized Al Kα radiation (1486.6 eV) using a PHI 5600ci ESCA spectrometer. The energy spectra of the electrons were analysed by a hemi-spherical mirror analyser with an energy resolution of about 0.4 eV. The Fermi level was referred to the gold 4f binding energy at 84 eV. The RMn_2 compounds proved to be very reactive. It was difficult to perform the measurements of the polycrystalline samples because of an oxygen and carbon contamination between the grains; it was impossible to remove this by sputtering with the argon ion beam. The single-crystalline samples produce spectra without or with little contamination by oxygen after breaking them under high vacuum and short subsequent sputtering. The measurements were made with a relatively short acquisition time because of the growing of the oxygen peak even under high-vacuum conditions (10^{-10} Torr).

The electrical resistivity measurements were performed by the conventional method using 100 mA DC current in the temperature range 4.2–300 K.

The measurements of the $GdMn_2$ magnetization were performed in the International Laboratory of High Fields and Low Temperature in Wrocław using static fields up to 140 kOe and pulsed fields up to 300 kOe along the principal and the [111] direction.

3. Results

3.1. Electronic structure

The spectra of $GdMn_2$ and YMn_2 in a wide range of binding energies are shown in figures 2 and 3. They are free from the contribution of oxygen and carbon contamination. The valence band of $GdMn_2$ together with Gd 4f and Gd 5p in comparison with pure Gd exhibits the domination of the Mn 3d states at the Fermi level (figure 4). The Gd 4f and 5p states in the compound are slightly shifted to a higher binding energy in comparison with pure Gd (about 0.5 eV) probably due to a chemical shift connected with the different chemical environment in the compound. The valence bands of YMn_2, $GdMn_2$, $ErMn_2$, YMn_4Al_8, $GdMn_4Al_8$, pure Mn and Gd are collected in figure 5. The common feature of the valence bands for all compounds is the pronounced character of the Mn 3d states which are hybridized with 4d states of yttrium or 5d states of gadolinium or erbium. All compounds have been measured at room temperature in the paramagnetic state. This state for YMn_2 is characterized as a weakly itinerant antiferromagnetism [21]. For $GdMn_2$ and YMn_2 the narrowing of the 3d states at the Fermi level is observed in comparison with pure manganese. For $ErMn_2$ (figures 6, 7) which crystallizes in a hexagonal structure and where the localized moments of Mn do not occur due to the small Mn–Mn distance, the valence band is less intensive, flatter and shifted from the Fermi level to a higher binding energy; this indicates the lower density

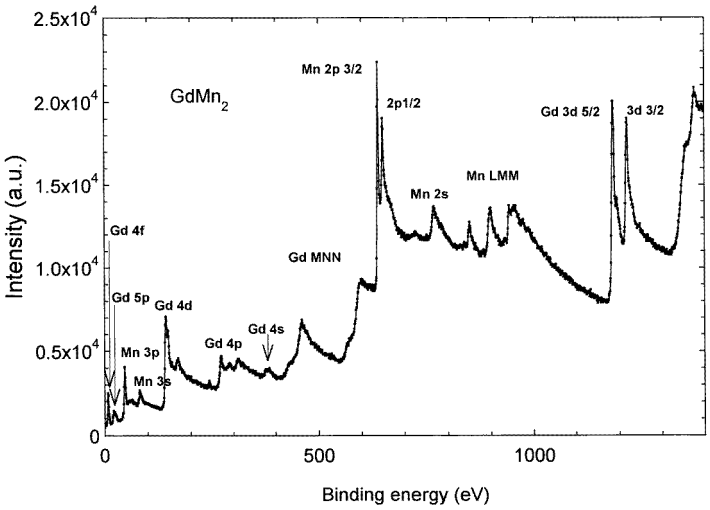

Figure 2. XPS spectrum of $GdMn_2$ in the wide range 0–1400 eV.

of states at the Fermi level. For YMn_2 the bandwidth of the valence states is comparable with pure Mn (above 4 eV). Beside the narrow peak close to the Fermi level (binding energy 0.7 eV), the second peak at about 2.7 eV is well defined. The splitting between Mn 3d peaks is about 2 eV. According to Himpsel [22] the exchange splitting of the 3d states near the Fermi level is found to be proportional to the local magnetic moment in a 3d metal, with a proportionality constant of 1 eV μ_B^{-1}. This correlation between the magnetic splitting and the magnetic moment is valid not only for ferromagnetic systems but also for antiferromagnetics. Deportes *et al* [23] examined the spin fluctuations in the paramagnetic state of YMn_2 using the polarized neutrons. They revealed the strong antiferromagnetic correlations which persisted up to $3T_N$. The value of the magnetic moment found at $3T_N$ (300 K) was 1.9 ± 0.1 μ_B in good agreement with the value of the exchange splitting in YMn_2 found in the XPS valence band at room temperature. For $GdMn_2$ the exchange splitting of Mn 3d was not observed perhaps because of the quenching of the spin fluctuation on manganese by gadolinium [24]. For $ErMn_2$ the exchange splitting was very weak (about 1 eV). For YMn_4Al_8 and $GdMn_4Al_8$ the valence band did not show any exchange splitting.

For pure Mn these two peaks are hardly distinguishable, they are much flatter and wider; this influences the properties and causes only the itinerant character of 3d electrons. The double-peaked DOS of d electrons for the YMn_2 compound was calculated by Yamada and Shimizu [14]. They explained that the antiferromagnetism of YMn_2 is mainly caused by the minority spin band of the d electrons at the Fermi level. The main part of the majority spin band lies below the Fermi level. This fact is responsible for the strong antiferromagnetism and the small value of the parallel susceptibility because d electrons cannot flip their spins too much with the external magnetic field. The described calculations are in good agreement with the measured valence band of YMn_2. For YMn_4Al_8 and $GdMn_4Al_8$ where Mn is non-magnetic the valence band is less intensive, flat and shifted towards higher binding energy similar to $ErMn_2$. However, for $ErMn_2$ a weak splitting and narrowing of the 3d states, as compared with YMn_4Al_8 and $GdMn_4Al_8$, is observed and spin fluctuations exist [25].

The core level states Mn 3s of $GdMn_2$ and YMn_2 (figure 8) exhibit similar exchange splitting as pure Mn; it equals about 4 eV. For YMn_4Al_8 and $GdMn_4Al_8$, where the manganese moment does not occur, this splitting is not observed.

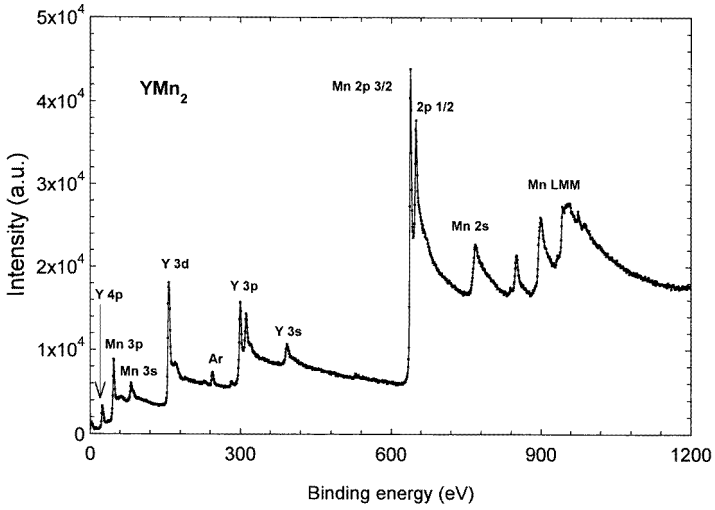

Figure 3. XPS spectrum of YMn_2 in the wide range 0–1200 eV.

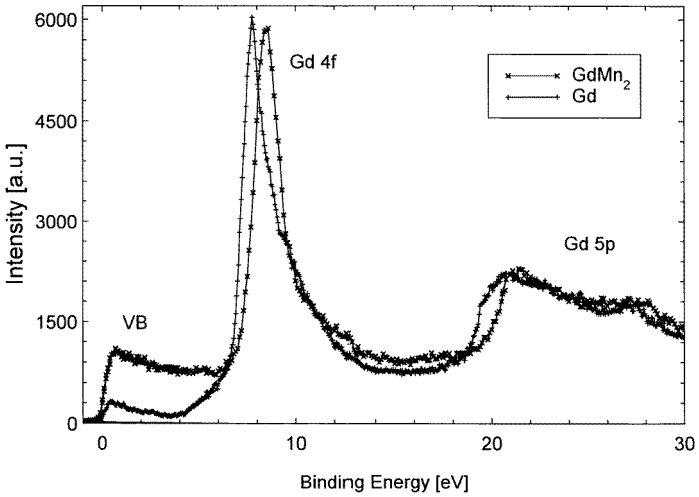

Figure 4. Valence band, Gd 4f and Gd 5p states of $GdMn_2$ and Gd.

3.2. Electrical resistivity

The electrical resistivity of $GdMn_2$ was measured on the single-crystalline sample along the growth direction [111] (figure 9). On cooling the electrical resistivity shows a rapid change at 118 K followed by the wide peak connected with the antiferromagnetic ordering of the Mn sublattice at 108 K. The second transition is observed at 32 K and may be related to the end of the magnetic or crystallographic transformation. In addition, an increase of the resistivity below 20 K was observed. The heating process exhibits the transition at 32 K and indicates a weak thermal hysteresis of the resistivity. Next, a rapid change of the resistivity with the very sharp antiferromagnetic peak and a wide thermal hysteresis

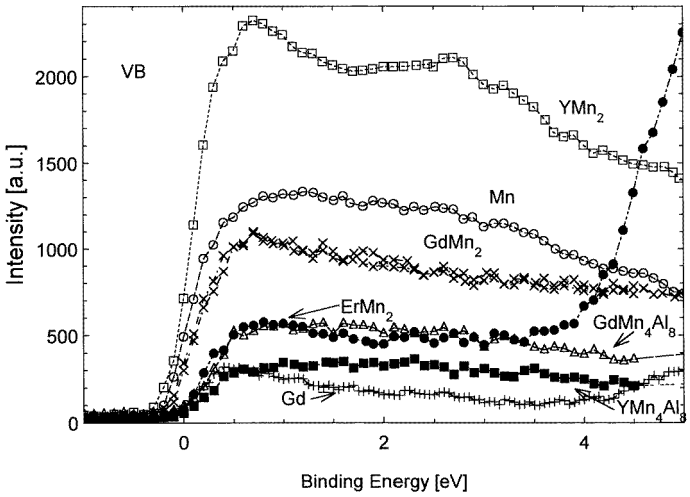

Figure 5. Valence bands of YMn_2, $GdMn_2$, $ErMn_2$, $GdMn_4Al_8$, YMn_4Al_8, Mn and Gd.

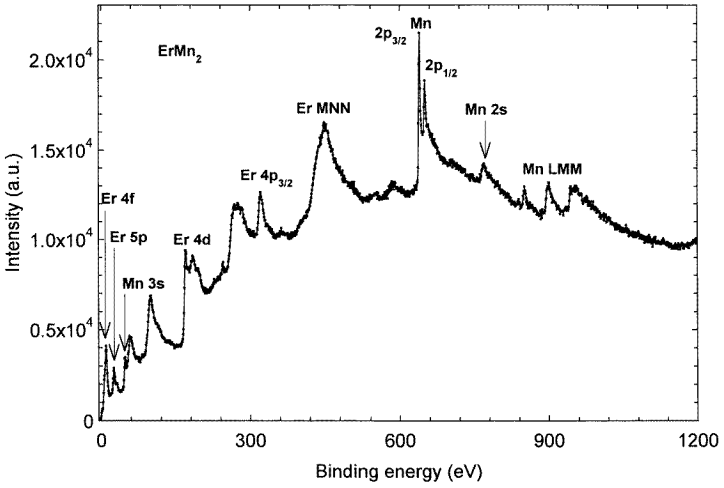

Figure 6. XPS spectrum of $ErMn_2$ in the wide range 0–1200 eV.

is observed at 108 K. After a strong volume transformation small amounts of the sample surface had peeled off, giving irregularities in the resistivity run.

3.3. Lattice parameter

In the whole temperature range $GdMn_2$ has the cubic C15 type structure. The temperature dependence of the lattice parameter of the $GdMn_2$ single crystals (figure 10) shows the beginning of the transition at 140 K on cooling. From the temperature of about 120 K the lattice parameter increases and a rapid change occurs at 110 K which is consistent with x-ray powder diffraction data [26] and the dilatometer measurements of the thermal expansion [8]. On heating the weak thermal hysteresis is observed up to the transition

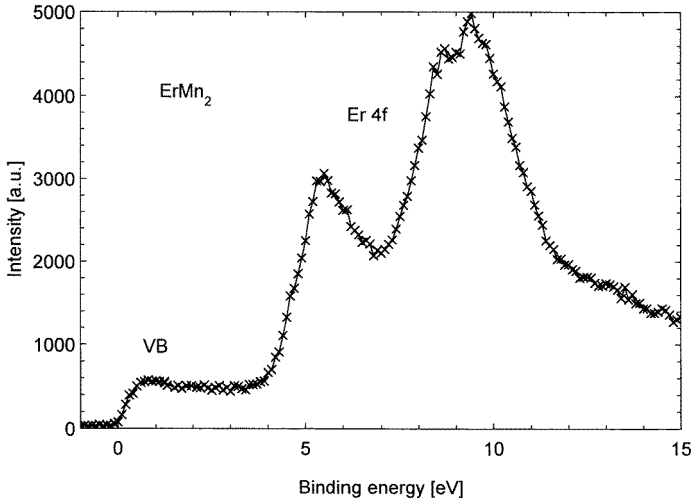

Figure 7. Valence band and Er 4f states of $ErMn_2$.

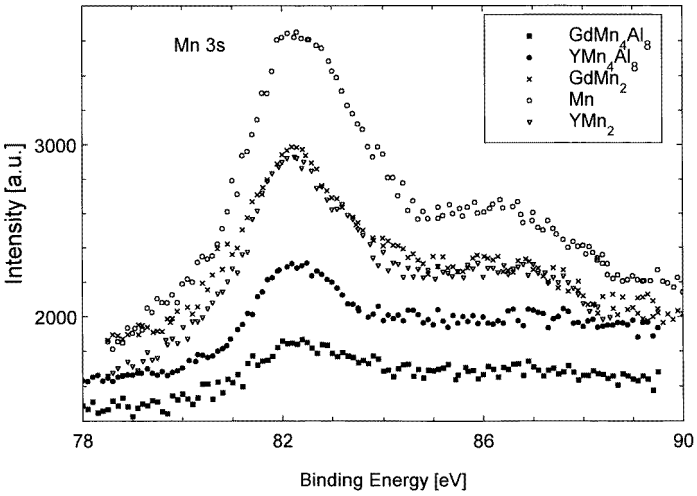

Figure 8. 3s states of YMn_2, $GdMn_2$, $GdMn_4Al_8$, YMn_4Al_8 and Mn.

region. The solid curve presents the hypothetical nonmagnetic behaviour calculated from the Grüneisen–Debye theory using $\Theta_D = 270$ K [27]. This discrepancy indicates that a spontaneous positive and temperature dependent magnetostriction takes place. The second smaller change is observed at about 30 K but it is within the error limit.

3.4. Magnetization

The magnetization measurements of a $GdMn_2$ single crystal along the principal direction [100] and along the [111] direction in the static fields show a strong anisotropy (figure 11). At 4.2 K and in the field of 150 kOe along [100] the value of the magnetization is close to zero; it is equal to only 0.2 μ_B fu^{-1} Along [111] the magnetization reaches 4.5 μ_B fu^{-1} at

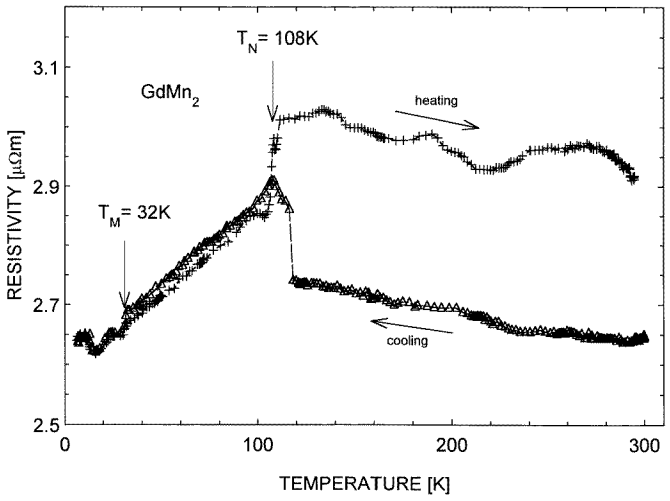

Figure 9. Temperature dependence of the electrical resistivity of $GdMn_2$ single crystal.

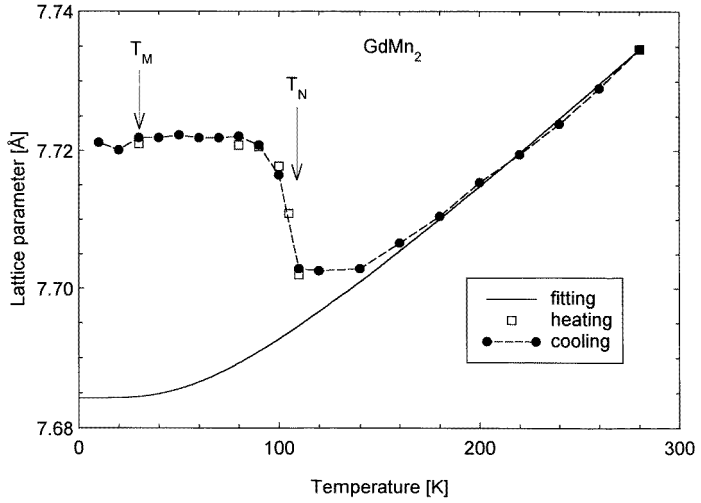

Figure 10. Temperature dependence of the lattice parameter of $GdMn_2$ single crystal and the theoretical fitting.

150 kOe and 4.2 K and appears far from saturation. The saturation effect was obtained in the pulsed fields up to 290 kOe with the value of the magnetic moment 5.2 μ_B fu^{-1} at 4.2 K (figure 12). Such a value of the magnetic moment in relatively high magnetic fields indicates the existence of the antiferromagnetic moment contribution of Mn. Assuming the antiparallel and canted arrangement of the Mn atoms [11, 14] and taking the magnetic moment of Mn as 3 μ_B and of Gd as 7 μ_B we can estimate 7 $\mu_B - 5.2$ $\mu_B = 1.8$ μ_B as a contribution of two manganese atoms to the magnetization. For one Mn (0.9 $\mu_B/3$ μ_B) = 0.3, which gives an angle $2\alpha = 145^\circ$ between Mn atoms.

The measurements of the magnetic moment versus temperature (figure 13) exhibit the ferromagnetic character of the magnetization with a very small value of the magnetic

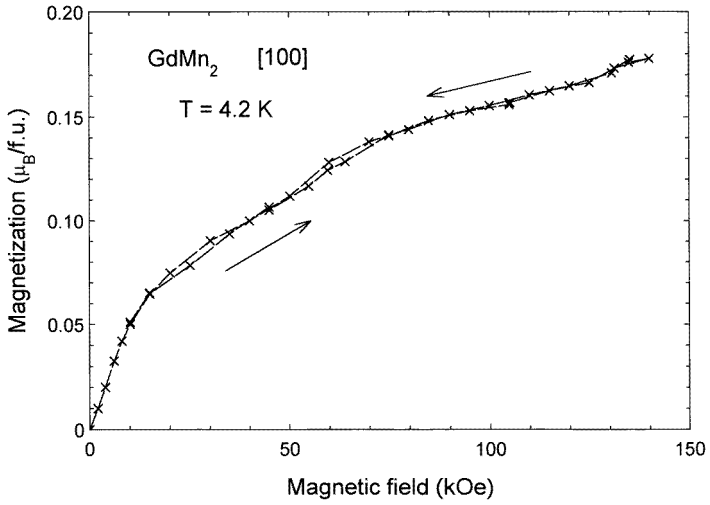

(a)

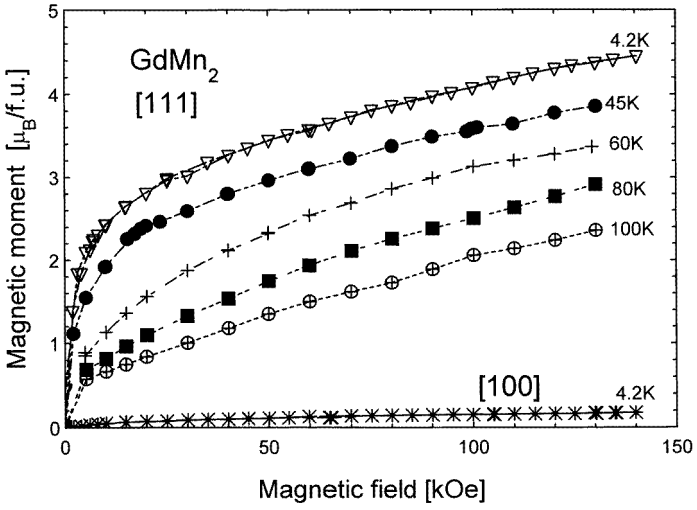

(b)

Figure 11. (a) Magnetization of $GdMn_2$ along the [100] direction in static fields. (b) Magnetization of $GdMn_2$ along the [111] direction in static fields.

moment (2.5 and 1.4 μ_B fu^{-1} in the fields 2 kOe and 10 kOe). In the weaker field of 2 kOe the additional transition at about 50 K is visible.

4. Discussion

The shape of the density of states at the Fermi level influences the magnetic properties of the measured compounds. It is correlated with the distance between the 3d atoms. The XPS measurements of RMn_2 and RMn_4Al_8 compounds show the change of the valence band with a decrease of this distance below the critical one when the manganese atoms

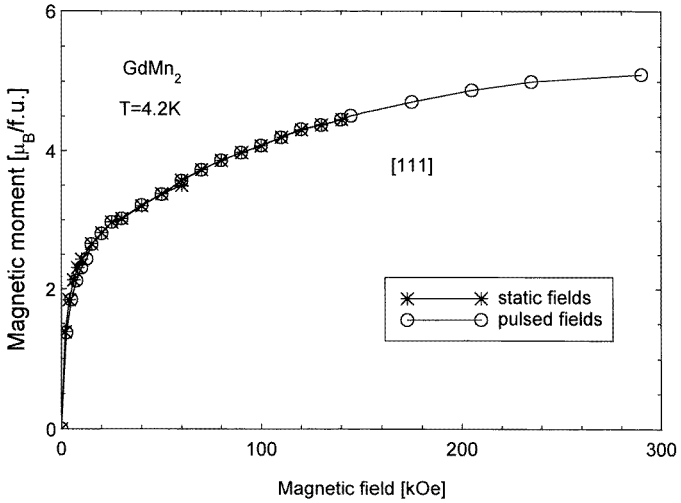

Figure 12. Magnetization of $GdMn_2$ along the [111] direction in pulsed fields.

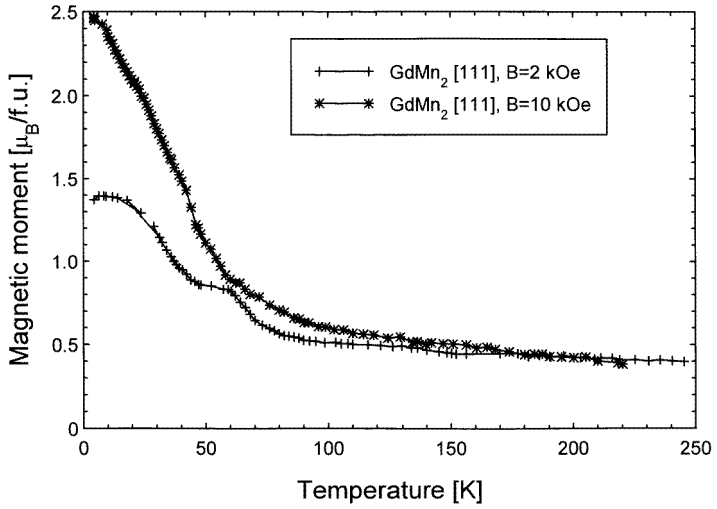

Figure 13. Temperature dependence of the $GdMn_2$ magnetization along the [111] direction at 2 and 5 kOe.

become weakly magnetic (for $ErMn_2$) or nonmagnetic (for YMn_4Al_8 and $GdMn_4Al_8$). The valence band at the Fermi level becomes wider, shifted to higher binding energies and less intense. This is because the interatomic d hopping integrals of d electrons and hence the d bandwidths are inversely proportional to the fifth power of the distance between the atoms [16]. Moreover the density of states at the Fermi level decreases so the intensity becomes lower. The exchange splitting of the core level Mn 3s is not sensitive to the change of the environment from pure Mn to RMn_2, which is similar to the results obtained by Arrot *et al* [28]. The valence band measurements are in agreement with the DOS calculated for YMn_2 by Yamada and Shimizu [16]. They also predicted the magnetic structure of $GdMn_2$ [14]. In this model the Mn atoms are canted by the hybridization between the 3d states of Mn and

the 5d states of the Gd atoms and by the exchange fields created by the localized moments of Gd. The resultant component of the canted and antiferromagnetically coupled Mn moments is antiparallel to the localized Gd moments. This produces a rather small total magnetic moment of $GdMn_2$ as compared to the free moment of the Gd^{3+} ion which is observed in the field dependent magnetization measurements. The angle between the canted Mn atoms may be sensitive to the change of the magnetic field and temperature; this results in the different antiferromagnetic contribution to the total magnetic moment. For $GdMn_2$ the easy direction was found as [111] similarly to YMn_2 [29]. The transition below 50 K observed in the resistivity, the lattice parameter and the magnetization versus temperature seems to be related to the canting process rather than to the ferromagnetic ordering of the Gd sublattice according to the lack of an anomaly in this region in the heat capacity measurements [12].

5. Conclusions

- The single crystals of YMn_2, $GdMn_2$, $ErMn_2$, YMn_4Al_8 and $GdMn_4Al_8$ were obtained by the Czochralski method from a levitated melt.
- The electronic structure shows the domination of Mn 3d states in the valence bands of the measured compounds. They hybridize with Y 4d or Gd, Er 5d states and clearly change their shape with the decrease of the critical distance d_c.
- The electrical resistivity of $GdMn_2$ exhibits the antiferromagnetic transition with the peak at $T_N = 108$ K and the second one at 32 K accompanied with a thermal hysteresis.
- The lattice parameter against temperature shows a C15 type of structure from 10 to 300 K and a large positive spontaneous magnetostriction at T_N.
- The magnetization reaches saturation at 290 kOe in the [111] direction with a magnetic moment of 5.2 μ_B fu^{-1}.
- The model of Yamada and Shimizu seems to be in agreement with the obtained results.
- Neutron measurement on single crystals are still highly desired.

Acknowledgments

This work is supported by KBN under project 2P 03B 135 08. ET is grateful to Osnabrück University for the possibility of the XPS measurements. The lattice parameter measurements of the single-crystals were made possible by the support of the Materialwissenshaftliches Forschungszentrum der Universität Mainz.

References

[1] Inoue K, Nakamura Y, Ikeda Y, Bando Y, Tsvyashenko A V and Fomicheva L 1995 *J. Phys. Soc. Japan* **64** 4901
[2] Wada H, Nakamura H, Yoshimura K, Shiga M and Nakamura Y 1987 *J. Magn. Magn. Mater.* **70** 70
[3] Kim-Ngan N H, Brommer P E and Franse J J M 1994 *IEEE Trans. Magn.* **MAG-30** 837
[4] Narasimha Rao C V, Wada H, Shiga M and Nakamura Y 1987 *J. Magn. Magn. Mater.* **70** 151
[5] Ballou R, Deportes J, Lemaire R, Nakamura Y and Ouladdiaf B 1987 *J. Magn. Magn. Mater.* **70** 129
[6] Shiga M, Wada H, Nakamura H, Yoshimura K and Nakamura Y 1987 *J. Phys. F: Met. Phys.* **17** 1781
[7] Shiga M 1994 *J. Magn. Magn. Mater.* **129** 17
[8] Makihara Y, Andoh Y, Hashimoto Y, Fuji H, Hasuo M and Okamoto T 1983 *J. Phys. Soc. Japan* **52** 629
[9] Ibarra M R, Marquina C, Garcia-Orza L, Arnold Z and del Moral A 1983 *J. Magn. Magn. Mater.* **128** L249
[10] Przewoźnik J, Żukrowski J and Krop K 1993 *J. Magn. Magn. Mater.* **119** 150
[11] Yoshimura K, Shiga M and Nakamura Y 1986 *J. Phys. Soc. Japan* **55** 3585
[12] Okamamoto T, Nagata H, Fujii H and Makihara Y 1987 *J. Magn. Magn. Mater.* **70** 139

[13] Żukrowski J, Kmieć R, Przewoźnik J and Krop K 1993 *J. Magn. Magn. Mater.* **123** L246
[14] Yamada H and Shimizu M 1986 *Phys. Lett.* **117** 313
[15] Yamada H and Shimizu M 1987 *J. Magn. Magn. Mater.* **70** 47
[16] Yamada H and Shimizu M 1987 *J. Phys. F: Met. Phys.* **17** 2249
[17] Hauser R, Ishii T, Sakai T, Oomi G, Uwatoko Y, Markosyan A S, Bauer E, Gratz E, Häufler T and Wiesinger G 1996 *J. Phys.: Condens. Matter* **8** 3095
[18] Coldea R, Coldea M and Pop I 1994 *IEEE Trans. Magn.* **MAG-30** 852
[19] Talik E, Szade J, Heimann J, Winiarska A, Winiarski A and Chełkowski A 1988 *J. Less-Common Met.* **138** 129
[20] *STAD* 14 1995 *Software Manual* (STOE & Cie GmbH)
[21] Yoshimura K, Takigawa M, Yasuoka H, Shiga M and Nakamura Y 1986 *J. Magn. Magn. Mater.* **54–57** 1075
[22] Himpsel F J 1991 *J. Magn. Magn. Mater.* **102** 261
[23] Deportes J, Ouladdiaf B and Ziebeck K R A 1987 *J. Magn. Magn. Mater.* **70** 14
[24] Coldea M 1996 private communication
[25] Wada H, Nakamura H, Yoshimura K, Shiga M and Nakamura Y 1987 *J. Magn. Magn. Mater.* **70** 134
[26] Tagawa Y, Sakurai J, Komura Y, Wada H, Shiga M and Nakamura Y 1985 *J. Phys. Soc. Japan* **54** 591
[27] Ślebarski A 1980 *J. Less-Common Met.* **72** 231
[28] Arrott A S, Heinrich B, Liu C and Purcell S T 1986 *J. Magn. Magn. Mater.* **54–57** 1025
[29] Yoshimura K and Nakamura Y 1983 *J. Magn. Magn. Mater.* **40** 55